

Article

# Formation of Anti-Wear Tribofilms via $\alpha$ -ZrP Nanoplatelet as Lubricant Additives

Wei Dai <sup>1</sup>, Bassem Kheireddin <sup>2</sup>, Hong Gao <sup>2</sup>, Yuwei Kan <sup>3</sup>, Abraham Clearfield <sup>3</sup> and Hong Liang <sup>1,\*</sup>

<sup>1</sup> Department of Mechanical Engineering, Texas A & M University, College Station, TX 77843, USA; daiwei7@gmail.com

<sup>2</sup> Shell Technology Center, Houston, TX 77082, USA; Bassem.Kheireddin@shell.com (B.K.); Hong.Gao@shell.com (H.G.)

<sup>3</sup> Department of Chemistry, Texas A & M University, College Station, TX 77843, USA; yuwei.kan@chem.tamu.edu (Y.K.); clearfield@chem.tamu.edu (A.C.)

\* Correspondence: hliang@tamu.edu; Tel.: +1-979-422-2480

Academic Editors: Antolin Hernández Battez, Rubén González Rodríguez and James E. Krzanowski

Received: 26 April 2016; Accepted: 29 July 2016; Published: 5 August 2016

**Abstract:** Effective tribofilms are desirable to protect mechanical systems. In the present research, we investigated the formation of a tribofilm through the use of  $\alpha$ -ZrP ( $\text{Zr}(\text{HPO}_4)_2 \cdot \text{H}_2\text{O}$ ) as an additive. Experiments were conducted on a base oil where 0.2 wt% of the additive was used. Experimental results showed a 50% reduction in friction and a 30% reduction in wear when compared to the base oil containing 0.8 wt% ZDDP. Spectroscopic characterization indicated that the tribofilm consists of iron oxide, zirconium oxide, and zirconium phosphates. The worn surface was seen to be smooth which renders it desirable for bearing systems.

**Keywords:** nanolubricants; tribofilms; friction; wear

## 1. Introduction

Since its discovery, Zinc dialkyl-dithiophosphate (ZDDP) has been used as the main anti-wear lubricant additive for almost a century. However, its potential to poison the vehicle emission catalyst raised environmental concerns and prompted the need for more eco-friendly lubricants. In general, lubricant additives include antioxidants, anti-wear additives, corrosion inhibitors, dispersants, defoamants, pour point depressants, viscosity modifiers, among others [1], and are used to compensate for the deficiencies of the base oil. Among those, ZDDP has been widely used because of its antiwear characteristics [2], which are largely due to the formation of a phosphate-based tribofilm. Phosphorus, however, has been reported to be damaging not only to the converter catalyst in engine emissions, but also to the environment in general. Efforts continue to be made to find suitable alternatives or to reduce its content. In addition, the low thermal stability of ZDDP leads to staining of metal surfaces [2]. Therefore, it is highly desirable to develop new lubricant additives with reduced phosphorus content.

In recent years, various novel lubricant additives have been developed, including nanoparticles, ionic liquids, and organic additive derivatives. Under different working conditions, those additives form tribofilms. A brief review was conducted, and a list of such additives is summarized in Table 1. As seen, the majority of these additives contain a high content of phosphate and sulfur compounds, which are not favorable for the environment.

**Table 1.** Properties of tribofilm formed by different additives.

Materials	Base Stock	Counterpart	Chemical Composition	Film Thickness	Mechanical Properties	Tribological Performance	Characterization Method	Reference
boron based additives	5W-30	E52100	Ca, O, S, B, Cr and ~40 at. % Fe	15 nm		friction and wear reduction	atom-probe tomography and TEM	[3]
Phosphate additives, AD and JD	triethanolamine aqueous solution	GCr15 bearing steel	P is in the form of phosphate or polyphosphate; S mainly exists as FeSO <sub>4</sub> and FeS <sub>2</sub>			friction and wear reduction	XPS and XANES	[4]
S-based EP additive and MoDTC additive	PAO	nc-WC/a-C(Al) carbon-based nanocomposite coating	WS <sub>2</sub> or MoS <sub>2</sub> + WS <sub>2</sub> -containing tribofilm		hardness (H) = 18.3 GPa, elastic modulus (E) = 213.1 GPa, critical load (Lc) = 28 N	Superior low-friction and anti-wear behaviors	XPS and TEM	[5]
attapulgit powder (silicate composed of some oxide)	mineral lubricating oil (150SN)	52100 steel and 1045 steel	FeO, Fe <sub>2</sub> O <sub>3</sub> , FeOOH and SiO <sub>x</sub>			friction and wear reduction	EDS and XPS	[6]
IL [P66614] [DEHP]	Chevron 15W40 and 0W30	steel-steel and silicon nitride-steel	metal phosphates and oxides	25 nm		wear reduction	EDS, XPS and TEM	[7]
Dithiocarbamate derivative additives	HVI WH150	GCr15 bearing steel and AISI 52100 steel	organic sulphide, pyrite, sulphite, -SC(=S)-N- part			better antiwear performance and extreme pressure property	XANES	[8]
Halogen-free borate ionic liquids		AISI 52100 steel-steel	phosphate based tribofilm			friction and wear reduction	XPS	[9]
IF-MoS <sub>2</sub>	blend of PAO 4 and PAO 40	AISI 52100 steel-steel	iron oxide and sulfides, MoS <sub>2</sub> ,	50–100 nm		friction and wear reduction	XPS and FIB	[10]
calcium sulphonate	PAO	aluminium-silicon and chromium steel	calcium carbonate and sulphur			wear reduction	ToF-SIMS	[11]
borate ester containing nitrogen	PAO	nitrided AISI 52100 steel	hexagonal BN and B <sub>2</sub> O <sub>3</sub>			friction reduced by 34% and wear reduced by 45%	XPS	[12]

Table 1. Cont.

Materials	Base Stock	Counterpart	Chemical Composition	Film Thickness	Mechanical Properties	Tribological Performance	Characterization Method	Reference
oleic acid-modified serpentine UFPs	mineral base oil (500SN)	GCr15 steel ball and 1045 steel disc	$\text{Fe}_3\text{O}_4$ , FeSi, $\text{SiO}_2$ , AlFe, and $\text{Fe}_3\text{C}$	500–600 nm	hardness = 8 GPa within 100 nm, modulus = 240 GPa within 100 nm	friction and wear reduction	EDS, TEM	[13]
serpentine powder	5-CST oil	GCr15 bearing steel	iron oxides, silicon oxides, magnesium oxides and organic compounds			friction and wear reduction	XPS and XANES	[14]
Cu nanoparticles and hydrosilicate powders	diesel oil	Ball AISI 52100 and Disk AISI 1045	iron oxides, silicon oxides, Si–O species, graphite, organic compounds, Cu species			friction and wear reduction	EDS and XPS	[15]

In our recent studies, we have discovered that when  $\alpha$ -ZrP nanoparticles were added into pure base oils, the friction and wear were significantly reduced. We have reported that amine intercalated  $\alpha$ -ZrP nanoparticles can reduce friction by more than 60% in a mineral oil [16,17]. To evaluate the viability of those particles in commercial based oils, the behavior of the additive in comparison with a commercially used additive, ZDDP, should be studied. In the present work, we focus on comparing their anti-wear behavior. The knowledge gained from this study is of great importance to the design of novel nanoparticle additives aimed at improving tribological performance.

## 2. Experimental Details

### 2.1. Materials

Synthesis of  $\alpha$ -ZrP nanoplatelets. Zirconyl chloride octahydrate (>99.0 wt%) was purchased from Fluka. Phosphoric acid (85 wt% in H<sub>2</sub>O) was purchased from Fisher-Scientific. The  $\alpha$ -ZrP nanoplatelets were synthesized by hydrothermal method reported by Sun and coworkers [18], and it has been described in our previous reports [16,17]. In summary, 4.0 g of ZrOCl<sub>2</sub>·8H<sub>2</sub>O was mixed well with 40.0 mL 12 M H<sub>3</sub>PO<sub>4</sub> in a sealed Teflon<sup>®</sup>-lined pressure vessel and heated at 200 °C for 24 h. The product was washed with deionized water and isolated by centrifuging five times at 5000 rpm, and dried at 70 °C for 24 h.

In this study, a base oil and ZDDP were provided by Shell Global Solutions (Houston, TX, USA). The base oil consists of hydrocarbon molecules without any additives. Its properties are similar to a light mineral oil. The concentrations of nanoplatelets and ZDDP in the base oil are 0.2 wt% and 0.8 wt%, respectively, corresponding to 0.02 wt% and 0.08 wt% phosphorus content.

### 2.2. Tribological Evaluation

Tribological evaluation was conducted using a pin-on-disk tribometer under room temperature. Bearing steel E52100 was used as pin (ball) ( $\varphi = 6$  mm) with surface roughness Ra<sub>1</sub> of 1.2  $\mu$ m. The same material was used as a substrate and has an Ra<sub>2</sub> of 0.01  $\mu$ m, resulting in a composite surface roughness of 1.2  $\mu$ m. Reciprocating sliding motion was configured in order to evaluate the wear behavior under a 5 N load (which corresponds to a maximum Hertzian pressure of 1 GPa) and a 1 Hz oscillation frequency. Wear track and sliding distance were set to 10 mm and 5000 m, respectively. The calculated oil film thickness is 0.04  $\mu$ m based on the Hamrock and Dowson formula [19]. Therefore, the theoretical lambda ratio is 0.03, which ensures boundary lubrication. Each test was repeated at least six times for repeatability. The cross-sectional profile of a wear track was obtained using a profilometer (KLA Tencor, Milpitas, CA, USA). The cross-sectional area was obtained through the profile data. It was measured at eight different positions on the wear track and the average and standard deviation were obtained. As a result, wear volume was calculated as the product of the wear track length and the cross-sectional area.

### 2.3. Characterization

After tribotests, the samples were rinsed with ethanol. The samples were then characterized using an optical microscope (Keyence VHX-2000, Osaka, Japan), SEM (Vega Tescan, Brno, Czech Republic, 10 KV, working distance is 15 mm), AFM (Nano-R2, Pacific Nanotechnology, Santa Clara, CA, USA, tapping mode) and XPS (Omicron, Taunusstein, Germany, Mg/Al X-ray source).

## 3. Results and Discussion

### 3.1. Friction and Wear

A significant reduction in friction was observed during pin-on-disk tribotests, as shown in Figure 1. The friction coefficient was plotted via the calculation of average value and standard deviation of multiple test results. In the case of the base oil (black squares) the process can be divided into three regimes. First, the friction coefficient reaches 0.22 at 1500 m which indicates the running-in

regime. It provides the highest friction coefficient throughout the process. By increasing sliding distance to 3500 m, the friction coefficient decreases gradually to 0.16 due to the increase in contact area. Under a constant load, the contact pressure decreases resulting in a lower friction. Eventually, the friction coefficient stabilizes, reaching a steady state. The base oil + ZDDP did not show the improved performance as seen in the case of  $\alpha$ -ZrP. In fact, the friction coefficient actually increased after a certain amount of time. This is consistent with the report that ZDDP increases friction due to the formation of a non-uniform tribofilm [20]. In the case of the base oil +  $\alpha$ -ZrP, as labeled by the blue triangles, it is clearly seen that the friction is reduced by nearly 50% compared to the base oil + ZDDP case. The short running-in period indicates the high working efficiency of  $\alpha$ -ZrP. We have recently reported the effective reduction of friction using sheet-like  $\alpha$ -ZrP nanoparticles in both mineral oil and water [16]. Within the boundary lubrication regime, two surfaces are closely in contact with each other. The sheet-like particles are able to separate the surfaces, thereby avoiding direct contact. The weak van der Waals force between the discs is responsible for promoting shear resulting in low frictional force. Similar results have been observed by other sheet-like particles, such as MoS<sub>2</sub> [21], H-BN [22], and WS<sub>2</sub> [23]. The present research further proves the effectiveness of nanosheets with weak interfacial bonding. It is noted that our experiments were conducted under a condition that we expected to generate some wear.

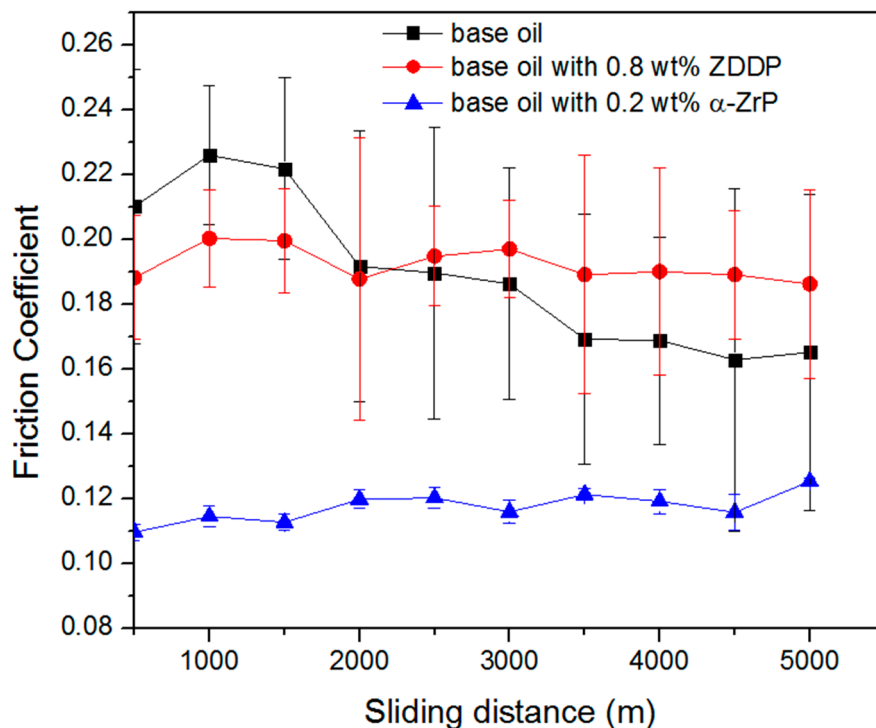
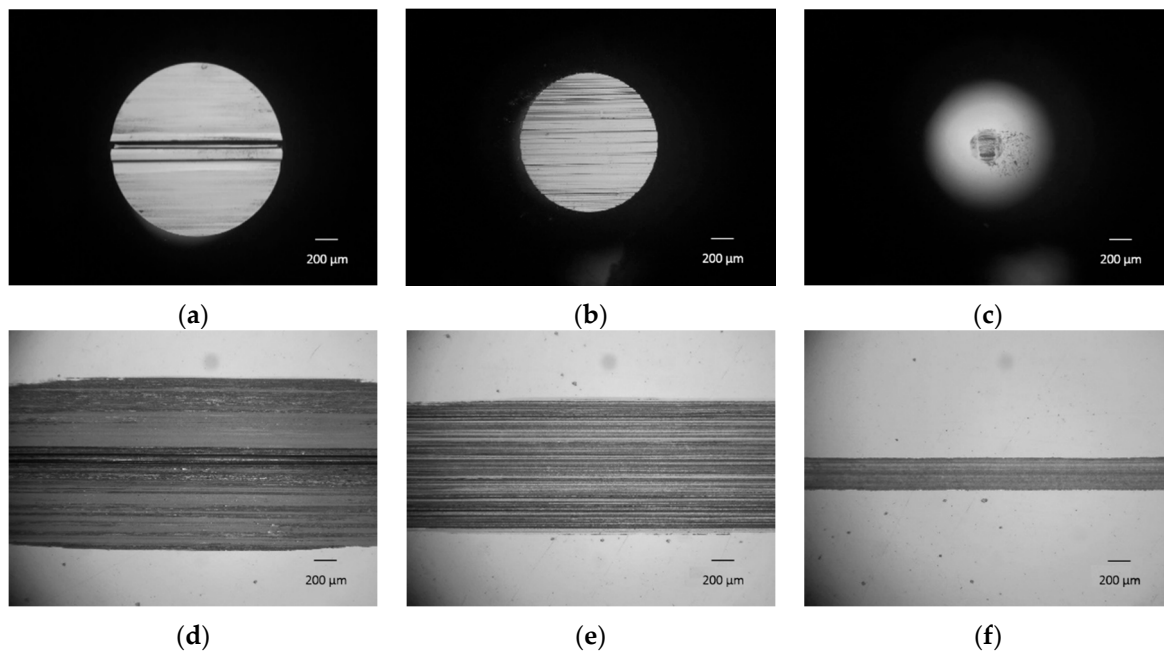


Figure 1. Friction coefficient changing with sliding distance.

The wear of rubbing surfaces with various lubricants was evaluated using an optical microscope. Figure 2 shows the optical images of the wear scar and the wear track. The diameter of the wear scar matches the width of the wear track, indicating a stable friction condition. A deep groove appeared on the wear scar of the base oil sample with a diameter of 1.47 mm. With the addition of ZDDP, the wear scar diameter decreased to 1.12 mm and many scratches could be found along with the sliding direction. However, using the base oil +  $\alpha$ -ZrP yielded a much smaller wear scar diameter (~0.27 mm).



**Figure 2.** Optical image of the wear scar and the wear track: (a,d) base oil; (b,e) base oil + ZDDP; (c,f) base oil +  $\alpha$ -ZrP.

To further study the morphology of the worn surfaces, the wear tracks were characterized by SEM, as shown in Figure 3. A patch-like surface was observed in the deep groove of base oil sample, which indicates severe adhesive and abrasive wear. With the addition of ZDDP, no deep groove was observed, only some shallow scratches and pits, which suggests less wear. In contrast, the wear track of the base oil +  $\alpha$ -ZrP exhibits no obvious wear, resulting in a relatively smooth surface.

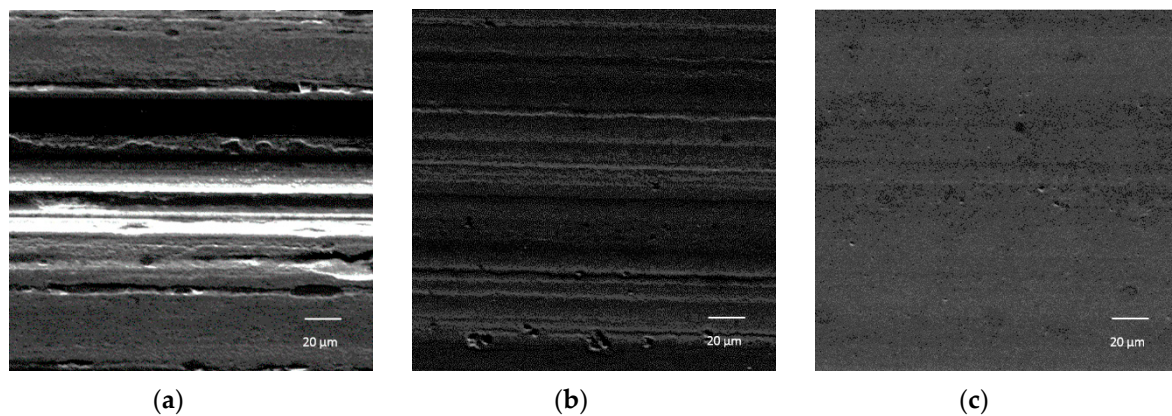


**Figure 3.** SEM image of the wear track: (a) base oil; (b) base oil + ZDDP; (c) base oil +  $\alpha$ -ZrP.

To compare the antiwear properties of ZDDP and  $\alpha$ -ZrP quantitatively, the wear track volume was measured by a profilometer as seen in Figure 4. Base oil +  $\alpha$ -ZrP shows nearly 30% wear reduction as compared with the base oil + ZDDP. Therefore, by combining the friction and wear results,  $\alpha$ -ZrP shows superior tribological performance.

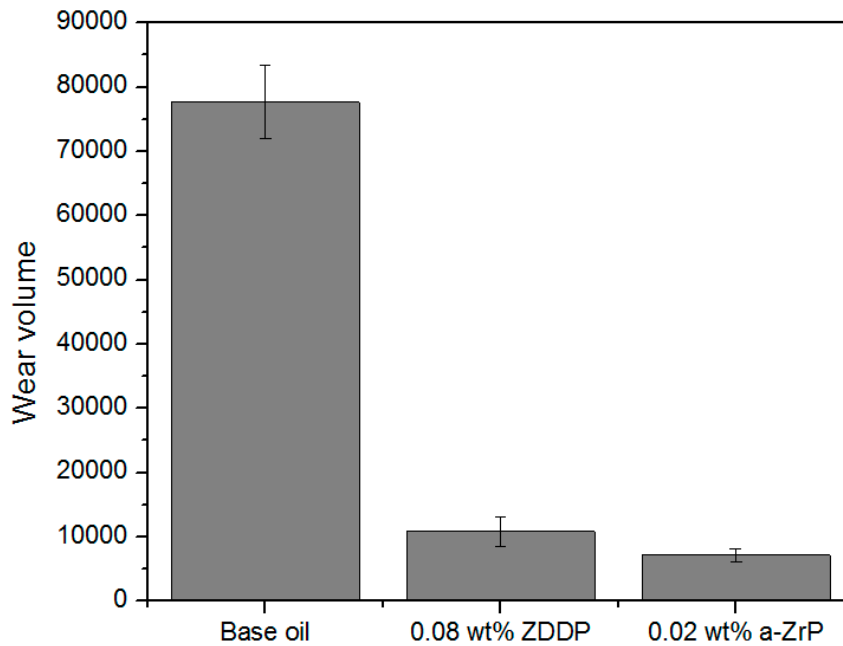


Figure 4. Volume of the wear track.

### 3.2. Tribofilm Formation

To understand the superior tribological performance of  $\alpha$ -ZrP, AFM was conducted on the wear track. The AFM scanning images are shown in Figure 5 and include: height images (Figure 5a–c), phase images (Figure 5d–f), and linear scan surface profiles across the wear track (Figure 5g–i). To compare the morphology of the wear track, the average surface roughness (Ra) and root mean square roughness (Rq) are listed in Table 2. As shown in Figure 5a, several grooves and a deep pit could be seen. The depth of the pit-like feature is roughly 600 nm (Figure 5g). The wear track of the base oil gives the highest surface roughness (271.03 nm). The height image of the base oil + ZDDP shows fewer asperities than that obtained from the base oil alone, with a peak-to-valley value of 448.3 nm. This surface has a slightly reduced surface roughness of 81.47 nm. On the other hand, the base oil +  $\alpha$ -ZrP has the smoothest surface with no visible asperities. Its phase image shows that this surface is smoother and more uniform than that obtained from the base oil + ZDDP (Figure 2d–f) with an average surface roughness of 40.89 nm. Based on this observation, both ZDDP and  $\alpha$ -ZrP could effectively reduce the surface asperities during the sliding process, but the wear track obtained with the base oil +  $\alpha$ -ZrP shows a significant effect on surface roughness reduction. The low and consistent friction coefficient is most likely related to the smooth wear track, as seen in Figure 2.

Table 2. Surface roughness parameters of the wear track.

Roughness Parameter	Base Oil	Base Oil + ZDDP	Base Oil + $\alpha$ -ZrP-ODI
Roughness Avg. (Sa)	271.03 nm	81.47 nm	40.89 nm
Root mean square (Sq)	315.73 nm	97.56 nm	59.02 nm

The iron spectrum can be deconvoluted as Fe 2p<sub>3/2</sub> and Fe 2p<sub>1/2</sub>. Two peaks in the Zr spectrum are due to Zr 3d<sub>3/2</sub> and Zr 3d<sub>5/2</sub>. Considering the O 1s peak at 529.5 eV and Fe 2p peak at 711.6 eV, the presence of Fe<sub>2</sub>O<sub>3</sub> could be confirmed. The O 1s peak at 529.5 eV and Zr 3d peak at 184.5 eV prove the presence of ZrO<sub>2</sub> [24]. Furthermore, the P 2p peak at 133 eV and Zr 3d peak at 184.5 eV show the existence of Zr(PO<sub>4</sub>)<sub>2</sub> [25]. ZrO<sub>2</sub> and Zr(PO<sub>4</sub>)<sub>2</sub> is a result of a tribochemical reaction. Thus the chemical composition of the tribofilm generated on the wear track may be composed of Fe<sub>2</sub>O<sub>3</sub>, ZrO<sub>2</sub>, and Zr(PO<sub>4</sub>)<sub>2</sub>.

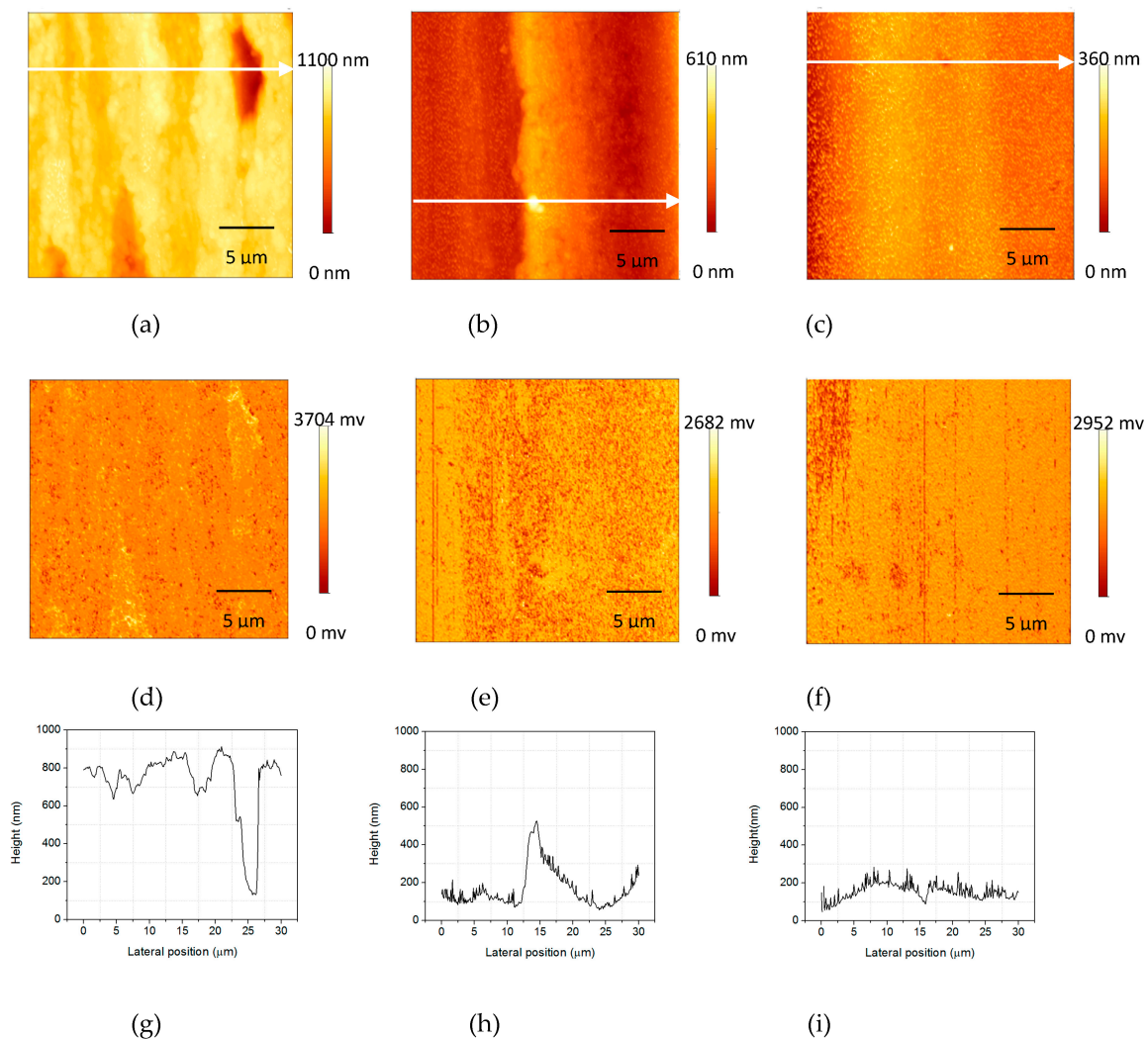


**Figure 5.** AFM height image, phase image and linear scan profile of the wear track: (a,d,g) base oil; (b,e,h) base oil + ZDDP; (c,f,i) base oil +  $\alpha$ -ZrP.

In order to analyze the chemical composition of the tribofilm, XPS analysis was conducted on the wear track. Figure 6 shows the XPS peaks of C 1s, O 1s, Fe 2p, Zr 3d, and P 2p for the tribofilms formed in the base oil +  $\alpha$ -ZrP. Peaks were deconvoluted using XPSpeak 4.1 software with an asymmetric Gauss-Lorentz profile after subtracting a Shirley background. The spectrum was calibrated by the C 1s peak at 284.6 eV.

In the following, the mechanisms of tribofilm formation are discussed. Nanoparticles morphologies and chemical compositions play significant roles in tribological performance and their effects have been studied systematically [26]. The sheet-like nanoparticles of  $\alpha$ -ZrP are found to be effective in friction and wear reduction. Due to their two-dimensional nature, the particles entered into the spatial area of contacting surfaces in the boundary lubrication regime. Due to their relatively large size on the disk surface, these particles are expected to effectively carry a load while the weak van der Waals force is responsible for a low shear force. According to the XPS spectra, the presence of a tribofilm was confirmed with the presence of tribochemical reaction products resulting from the reaction between the lubricant and the steel substrate.

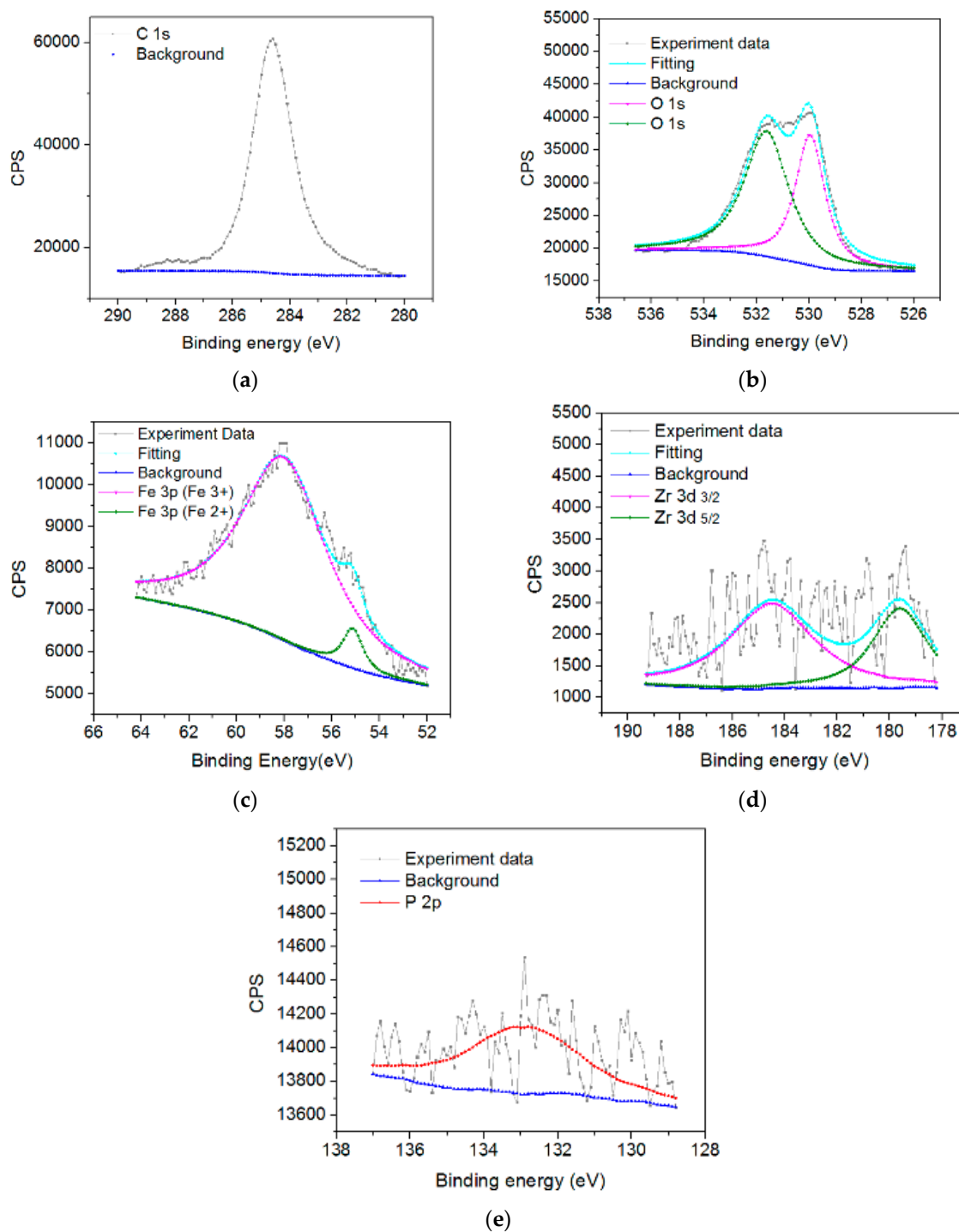


**Figure 6.** XPS spectrum of the base oil +  $\alpha$ -ZrP wear track. (a) C 1s; (b) O 1s; (c) Fe 3p; (d) Zr 3d and (e) P 2p.

The composition of the ZDDP tribofilm has been studied extensively and its major components are iron oxide, zinc oxide, phosphate compounds, and sulfides [27,28]. In the case of  $\alpha$ -ZrP, due to the low phosphorus content (200 ppm), zirconium compounds played an important role in wear protection rather than phosphate compounds. The tribological performance of  $ZrO_2$  nanoparticles was compared to ZDDP.  $ZrO_2$  acts as an abrasive and shows poor wear resistance during the sliding process. In the current research,  $ZrO_2$  was the tribochemical reaction product and was anchored in the tribofilm as a part of it. Unlike  $ZrO_2$  nanoparticles,  $ZrO_2$  in the tribofilm could not transition freely. Conversely, presence of  $ZrO_2$  increases the hardness of substrates, which leads to improved

wear resistance. As a result, the superior antiwear performance of the tribofilm is due to the synergetic effect of  $\text{Fe}_2\text{O}_3$ ,  $\text{ZrO}_2$ , and  $\text{Zr}(\text{PO}_4)_2$ . The sheet-like  $\alpha$ -ZrP is expected to effectively separate the two contacting surfaces in the boundary lubrication regime, thereby leading to less wear. Moreover, the reduced contact area indicates better load bearing capacity of the tribofilm. The summary comparison of the ZDDP and the  $\alpha$ -ZrP tribofilms is illustrated in Figure 7. The next step is to optimize the reduction of the friction coefficient through the base oil selection. The confirmation of formation of a quality tribofilm is a significant step in nanolubricants.

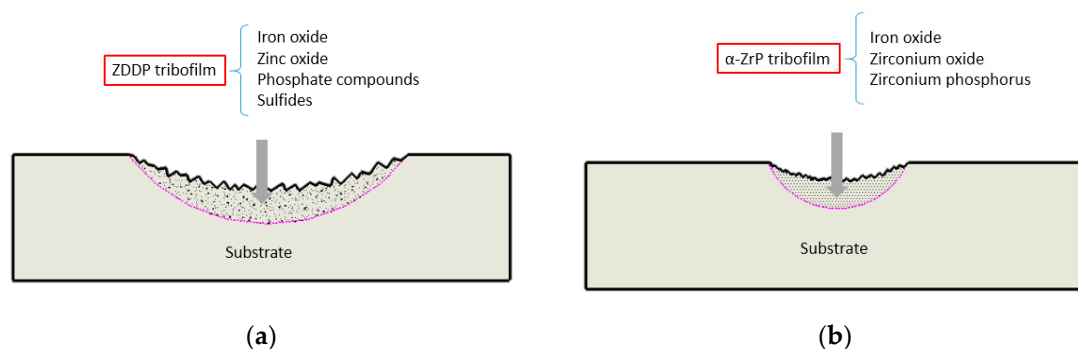


Figure 7. Schematic of the tribofilm composition of ZDDP (a) and  $\alpha$ -ZrP (b).

#### 4. Conclusions

In this research, an alternative nanolubricant is developed to replace commercial ZDDP-containing lubricants. We investigated the characteristics of the tribofilm formed through the addition of  $\alpha$ -ZrP nanoparticles in a reference oil. Tribological studies were carried out using a pin-on-disk configuration in a reciprocating motion. Experimental results showed superior tribological performance of the sheet-like nanoparticles: when compared with ZDDP,  $\alpha$ -ZrP showed a 50% reduction in friction and a 30% reduction in wear. XPS spectroscopic analysis indicates that an anti-wear tribofilm composed of  $\text{Fe}_2\text{O}_3$ ,  $\text{ZrO}_2$ , and  $\text{Zr}(\text{PO}_4)_2$  is formed. This zirconium based tribofilm is characterized by a lower surface roughness and an improved load bearing capability than the ZDDP tribofilm. The low-phosphorus-content-lubricant additives have strong potential as substitutes for ZDDP. Future studies will focus on the optimization of tribological performance.

**Acknowledgments:** The authors thank Kyungjun Lee for assistance in AFM analysis and Lian Ma for assistance in XPS analysis.

**Author Contributions:** Wei Dai performed experiments, analyzed data, and wrote the paper. Bassem Kheireddin and Hong Gao provided base oil and discussed results. Yuwei Kan synthesized nanoparticles. Abraham Clearfield edited the paper. Hong Liang conceived research, analyzed results, and wrote the paper.

**Conflicts of Interest:** The authors declare no conflict of interest.

#### References

1. Wills, J.G. *Lubrication Fundamentals*; Marcel Dekker Inc.: New York, NY, USA, 1980.
2. Spikes, H. The History and Mechanisms of ZDDP. *Tribol. Lett.* **2004**, *17*, 469–489. [[CrossRef](#)]
3. Kim, Y.-J.; Baik, S.-I.; Bertolucci-Coelho, L.; Mazzaferro, L.; Ramirez, G.; Erdermir, A.; Seidman, D.N. *Atom-Probe Tomography of Tribological Boundary Films Resulting from Boron-Based Oil Additives*; Scripta Materialia: Columbus, OH, USA, 2015.
4. Ma, H.B.; Li, J.; Chen, H.; Zuo, G.Z.; Yu, Y.; Ren, T.H.; Zhao, Y.D. XPS and XANES characteristics of tribofilms and thermal films generated by two P- and/or S-containing additives in water-based lubricant. *Tribol. Int.* **2009**, *42*, 940–945. [[CrossRef](#)]
5. Zhou, S.G.; Wang, L.P.; Xue, Q.J. Controlling friction and wear of nc-WC/a-C(AI) nanocomposite coating by lubricant/additive synergies. *Surf. Coat. Technol.* **2012**, *206*, 2698–2705. [[CrossRef](#)]

6. Nan, F.; Xu, Y.; Xu, B.S.; Gao, F.; Wu, Y.X.; Tang, X.H. Effect of natural attapulgite powders as lubrication additive on the friction and wear performance of a steel tribo-pair. *Appl. Surf. Sci.* **2014**, *307*, 86–91. [[CrossRef](#)]
7. Cai, Z.-B.; Meyer, H.M., III; Ma, C.; Chi, M.; Luo, H.; Qu, J. Comparison of the tribological behavior of steel–steel and Si<sub>3</sub>N<sub>4</sub>–steel contacts in lubricants with ZDDP or ionic liquid. *Wear* **2014**, *319*, 172–183. [[CrossRef](#)]
8. Fan, K.Z.; Li, J.; Ma, H.B.; Wu, H.; Ren, T.H.; Kasrai, M.; Bancroft, G.M. Tribological characteristics of ashless dithiocarbamate derivatives and their combinations with ZDDP as additives in mineral oil. *Tribol. Int.* **2008**, *41*, 1226–1231. [[CrossRef](#)]
9. Totolin, V.; Minami, I.; Gabler, C.; Doorr, N. Halogen-free borate ionic liquids as novel lubricants for tribological applications. *Tribol. Int.* **2013**, *67*, 191–198. [[CrossRef](#)]
10. Rabaso, P.; Ville, F.; Dassenoy, F.; Diaby, M.; Afanasiev, P.; Cavoret, J.; Vacher, B.; Le Mogne, T. Boundary lubrication: Influence of the size and structure of inorganic fullerene-like MoS<sub>2</sub> nanoparticles on friction and wear reduction. *Wear* **2014**, *320*, 161–178. [[CrossRef](#)]
11. Burkinshaw, M.; Neville, A.; Morina, A.; Sutton, M. The lubrication of both aluminium-silicon and model silicon surfaces with calcium sulphonate and an organic antiwear additive. *Tribol. Int.* **2013**, *67*, 211–216. [[CrossRef](#)]
12. Wang, S.; Yue, W.; Fu, Z.Q.; Wang, C.B.; Li, X.L.; Liu, J.J. Study on the tribological properties of plasma nitrided bearing steel under lubrication with borate ester additive. *Tribol. Int.* **2013**, *66*, 259–264. [[CrossRef](#)]
13. Yu, H.L.; Xu, Y.; Shi, P.J.; Wang, H.M.; Wei, M.; Zhao, K.K.; Xu, B.S. Microstructure, mechanical properties and tribological behavior of tribofilm generated from natural serpentine mineral powders as lubricant additive. *Wear* **2013**, *297*, 802–810. [[CrossRef](#)]
14. Zhang, Y.; Li, Z.; Yan, J.; Ren, T.; Zhao, Y. Tribological behaviours of surface-modified serpentine powder as lubricant additive. *Ind. Lubr. Tribol.* **2016**, *68*, 1–8. [[CrossRef](#)]
15. Zhang, B.-S.; Xu, B.-S.; Xu, Y.; Gao, F.; Shi, P.-J.; Wu, Y.-X. CU nanoparticles effect on the tribological properties of hydrosilicate powders as lubricant additive for steel–steel contacts. *Tribol. Int.* **2011**, *44*, 878–886. [[CrossRef](#)]
16. He, X.L.; Xiao, H.P.; Choi, H.H.; Diaz, A.; Mosby, B.; Clearfield, A.; Liang, H. Alpha-Zirconium phosphate nanoplatelets as lubricant additives. *Colloid Surf. A* **2014**, *452*, 32–38. [[CrossRef](#)]
17. Xiao, H.P.; Dai, W.; Kan, Y.W.; Clearfield, A.; Liang, H. Amine-intercalated alpha-zirconium phosphates as lubricant additives. *Appl. Surf. Sci.* **2015**, *329*, 384–389. [[CrossRef](#)]
18. Sun, L.; Boo, W.J.; Sue, H.-J.; Clearfield, A. Preparation of  $\alpha$ -zirconium phosphate nanoplatelets with wide variations in aspect ratios. *New J. Chem.* **2007**, *31*, 39–43. [[CrossRef](#)]
19. Hamrock, B.J.; Dowson, D. *Ball Bearing Lubrication: The Elastohydrodynamics of Elliptical Contacts*; John Wiley & Sons: Hoboken, NJ, USA, 1981.
20. Taylor, L.; Spikes, H. Friction-enhancing properties of ZDDP antiwear additive: Part I—Friction and morphology of ZDDP reaction films. *Tribol. Trans.* **2003**, *46*, 303–309. [[CrossRef](#)]
21. Joly-Pottuz, L.; Dassenoy, F.; Belin, M.; Vacher, B.; Martin, J.M.; Fleischer, N. Ultralow-friction and wear properties of IF-WS<sub>2</sub> under boundary lubrication. *Tribol. Lett.* **2005**, *18*, 477–485. [[CrossRef](#)]
22. Pawlak, Z.; Kaldonski, T.; Pai, R.; Bayraktar, E.; Oloyede, A. A comparative study on the tribological behaviour of hexagonal boron nitride (h-BN) as lubricating micro-particles—An additive in porous sliding bearings for a car clutch. *Wear* **2009**, *267*, 1198–1202. [[CrossRef](#)]
23. Totolin, V.; Ripoll, M.; Jech, M.; Podgornik, B. Enhanced tribological performance of tungsten carbide functionalized surfaces via in-situ formation of low-friction tribofilms. *Tribol. Int.* **2016**, *94*, 269–278. [[CrossRef](#)]
24. Majumdar, D.; Chatterjee, D.; Ghosh, S.; Blanton, T. X-Ray Photoelectron Spectroscopic Studies on Ceramic Composites Containing Yttria-Stabilized Zirconia and Alumina. *Appl. Surf. Sci.* **1993**, *68*, 189–195. [[CrossRef](#)]
25. Arfelli, M.; Mattogno, G.; Ferragina, C.; Massucci, M.A. Xps Characterization of Gamma-Zirconium Phosphate and of Some of Its Intercalation Compounds—A Comparison with the Alpha-Zirconium Phosphate Analogs. *J. Inclusion Phenom. Mol.* **1991**, *11*, 15–27. [[CrossRef](#)]
26. Dai, W.; Kheireddin, B.; Gao, H.; Liang, H. Roles of nanoparticles in oil lubrication. *Tribol. Int.* **2016**, *102*, 88–98. [[CrossRef](#)]

27. Martin, J.M. Antiwear mechanisms of zinc dithiophosphate: A chemical hardness approach. *Tribol. Lett.* **1999**, *6*, 1–8. [[CrossRef](#)]
28. Zhou, Q.; Huang, J.; Wang, J.; Yang, Z.; Liu, S.; Wang, Z.; Yang, S. Preparation of a reduced graphene oxide/zirconia nanocomposite and its application as a novel lubricant oil additive. *RSC Adv.* **2015**, *5*, 91802–91812. [[CrossRef](#)]



© 2016 by the authors; licensee MDPI, Basel, Switzerland. This article is an open access article distributed under the terms and conditions of the Creative Commons Attribution (CC-BY) license (<http://creativecommons.org/licenses/by/4.0/>).